Illumination Induced Changes in Image Statistics

Thanh Bui, Reiner Lenz, Martin Solli
Department of Science and Technology, Linköping University
SE-60174 Norrköping, Sweden

Abstract

We have previously shown that it is possible to construct a coordinate system in the space of illumination spectra such that the coordinate vectors of the illuminants are located in a cone. Changes in the space of illuminants can then be described by an intensity related scaling and a transformation in the Lorentz group SU(1,1).

In practice it is often difficult and expensive to measure these coordinate vectors. Therefore it is of interest to estimate the characteristics of an illuminant from an RGB image captured by a camera. In this paper we will investigate the relation between sequences of illuminants and statistics computed from RGB images of scenes illuminated by these illuminants.

As a typical example we will study sequences of black body radiators of varying temperature. We have shown earlier that black body radiators in the mired parametrization can be described by one-parameter groups of the Lorentz group SU(1,1). In this paper we will show that this group theoretical structure of the illuminant space induces a similar structure in spaces of statistical descriptors of the resulting RGB images. We show this relation for mean vectors of RGB images, for RGB histograms and for histograms of images obtained by applying certain spatio-spectral linear filters to the RGB images. As a result we obtain estimates of the color temperature of the illuminant from sequences of RGB images of scenes under these illuminants.

Introduction

Understanding the relation between illumination, reflection and sensor properties is one of the most central and important problems in color imaging and color image processing. Typical applications where models that describe the interaction between these three factors are useful include: white balancing in digital cameras, understanding of the mechanisms behind color constancy in human perception and color information processing for pattern recognition and computer vision are some examples.

In our previous work we developed a geometrical framework for color signal processing (see [3, 5, 4]). In this framework we consider only single object points in isolation. A typical example is the description of the effects of illumination changes: Here we describe the spectral characteristics of the changing illumination by the spectral distributions of the illumination source. Such an illumination spectrum interacts with the reflectance spectrum of an object point generating the color signal. The color signal, in turn, interacts with the sensor (characterized by its sensitivity functions) and as a result a pixel vector is generated. This is repeated for all illumination sources and thus a sequence of pixels is generated that represent the color appearance of this object point under the illuminations as seen by the sensor.

This is obviously a very restrictive framework corresponding to the problem of analyzing the relation between the illumination and the reflection properties while being located in a room painted in a single (unknown) color. In reality this will almost never be the case since we can simultaneously observe the interaction between a large number of different reflectance spectra (representing different object points) and the illumination. From this we conclude that we can usually analyze a large number of object/illumination interactions simultaneously. A second observation is that we probably do not analyze these points individually but we can base our analysis on statistical properties of collections of such points.

In this paper we will thus generalize our previous work by analyzing the relation between illumination spectra, a sensor and statistical properties of the reflection spectra and the pixel vectors. We will show that the group theoretical structure in the space of illuminant spectra is mapped to similar structures in certain spaces derived from the RGB images showing a scene illuminated by different illumination sources. In the following section we will first give a brief description of the group theoretical background and the previous results regarding the illumination spectra. Then we will introduce the framework used in the rest of the text and finally we will describe the results of our experiments.

An Overview over Conical Color Spaces

We showed previously that it is possible to introduce a coordinate system in the space of illumination spectra such that the corresponding coordinate vectors are all located in a cone. This is a consequence of the restriction that all illumination spectra can only assume non-negative function values. The basic construction is as follows: Consider a collection of illumination spectra relevant for a given application. Compute the eigenvectors (belonging to the largest eigenvalues) of the correlation matrix and use them as basis vectors. Illumination spectra are now characterized by coordinate vectors that contain the expansion coefficients in this new coordinate system. This representation is the familiar principal component analysis (PCA). It can be shown that the first eigenvector has only non-negative values and that these coefficient vectors are all located in a cone. For many databases it can be shown that very few eigenvectors provide a sufficient description of the spectra of interest. In the following we will restrict us to systems consisting of three eigenvectors. The coordinate vectors are thus all located in a three-dimensional cone. We will use the following notation: we write vectors with the first three PCA-coefficients as (c_0, c_1, c_2). If s is the illumination spectrum, $b_k, k = 0, 1, \dots$ are the eigenvectors and $\langle ., . \rangle$ denotes the scalar product in the function space of illumination spectra then the coefficients are given by $c_k = \langle s, b_k \rangle$ leading to the approximation

$$s \approx \langle s, b_0 \rangle b_0 + \langle s, b_1 \rangle b_1 + \langle s, b_2 \rangle b_2 \qquad (1)$$

Instead of this "raw" coordinate vector we usually use the scalar c_0 and the complex number $z = x + iy$ with $x = c_1/c_0, y = c_2/c_0$. This is possible since $c_0 > 0$ (except for the perfect black illumination). Empirically it has been shown that c_0 is related to the intensity of the source and z to its chromaticity.

From mathematics and theoretical physics it is known that the conical structure of spaces is preserved by the so-called Lorentz-transformations. For geometrical reasons it is therefore interesting to investigate if the Lorentz-transformations applied to illumination spectra have an interpretation in terms of color science. As example consider a sequence of illumination spectra given by the black-body radiators. We describe the black-body radiator of temperature T (measured in Kelvin) by the spectral distribution $s(T)$, the PCA-coordinate vectors as $(c_0(T), c_1(T), c_2(T))$ and correspondingly $z(T)$ for the complex coordinates. The relevant Lorentz Group is in this case the group SU(1,1) consisting of the following 2x2 matrices:

$$SU(1,1) = \left\{ M = \begin{pmatrix} \alpha & \beta \\ \overline{\beta} & \overline{\alpha} \end{pmatrix} : \alpha, \beta \in \mathbb{C}; |\alpha|^2 - |\beta|^2 = 1 \right\} \tag{2}$$

For a matrix $M \in SU(1,1)$ and a complex number z with $|z| < 1$ we define the fractional linear transform:

$$M\langle z \rangle = \frac{\alpha z + \beta}{\overline{\beta} z + \overline{\alpha}} \tag{3}$$

Instead of using parameters α, β it is in our context more efficient to use an exponential construction. Define the following three matrices:

$$J_1 = \frac{1}{2} \begin{bmatrix} i & 0 \\ 0 & -i \end{bmatrix}; \quad J_2 = \frac{1}{2} \begin{bmatrix} 0 & 1 \\ 1 & 0 \end{bmatrix}; \quad J_3 = \frac{1}{2} \begin{bmatrix} 0 & i \\ -i & 0 \end{bmatrix} \tag{4}$$

For scalars ξ_1, ξ_2, ξ_3 we define:

$$X = \xi_1 J_1 + \xi_2 J_2 + \xi_3 J_3 \tag{5}$$

It can then be shown that e^X is an element in SU(1,1). Furthermore we find that for every (fixed) matrix X the matrices $\{e^{tX}, t \in \mathbb{R}\}$ form a so-called one-parameter subgroup. For a fixed X and a real value t we define

$$M_t = e^{tX} \tag{6}$$

With these notations we can now summarize our previous experiments with black-body radiators as follows: Denote by $z(T)$ the chromaticity coordinates of the black-body radiators as introduced above. Select a fixed temperature T_0 and write $z_0 = z(T_0)$. Then we can find a matrix X such that the curve $z(T)$ in the complex plane can be approximated by the curve $M_t \langle z_0 \rangle$. This approximation holds if we consider the two curves as sets of points. If we parameterize the curve in the complex plane by the inverse temperature, i.e. consider $z(1/T)$ then it can be shown that the exponential parameter t and the inverse temperature $1/T$ are almost linear functions of each other. This is interesting since human perception of color differences is also related to inverse temperature (see [9] and [10] pages 224-225).

Apart from the space of illumination spectra (with its conical shape) we need to consider two other function spaces: the space of reflection spectra and the space of color signals. A reflection spectrum is by definition a function $r(\lambda)$ where $r(\lambda)$ describes the probability that a photon of wavelength is reflected from the object. By definition we have $0 \leq r(\lambda) \leq 1$ and the space of reflection spectra forms an (infinite-dimensional) cube. A color signal is defined as the (pointwise) product between illumination spectra and reflection spectra, i.e. $c(\lambda) = r(\lambda)s(\lambda)$ and for a fixed, given illumination we can think of the space of

color signals as a copy of the conical space of illumination spectra. Another way to describe the same relation is to view the illumination spectrum s as an operator that maps one color signal space (the space of reflection spectra under perfect white illumination) to another color signal space (the space of reflection spectra under illumination s. We extend this to the whole color signal space and arrive at the following operator interpretation of the illuminant:

$$s : \mathscr{C} \to \mathscr{C}; c(\lambda) \mapsto c(\lambda) \cdot s(\lambda) \tag{7}$$

Here $\mathscr{C}$ is the space of color signals and we use s to denote both, the illumination spectrum and the corresponding operator. In the following we will study the behavior of operators derived from this operator.

The General Model

In the basic model the illumination spectrum defines an operator on the space of color signals. In almost all situations the illumination interacts not only with a single reflectance spectrum but with a large collection of reflectance points in a scene. The resulting collection of color signals will be measured with the help of sensors. In the case of human color vision the sensors are the receptors in the eye, in the case of technical systems the sensors are the chips in digital cameras or analog film. The result of this interaction between the color signals and the sensors is a color image. This transform from the space of color signals $\mathscr{C}$ to the space of images $\mathscr{I}$ is given by the first 'vertical' transformation in Figure 1. The same camera operator operates on the original color signals and on the color signals generated by the illumination operator s. As a result we see that the illumination operator s induces a new operator s_i on the space of images. This operator describes the change of images as a result of an illumination change.

In almost all imaging systems these raw measurements on the sensor level are followed by post-processing operations. In the case of human color vision typical post processing is done by the receptive fields. In the case of digital cameras post-processing consists of various types of demosaicing and image processing. Typical operations at that level are linear filter operations as indicated in the lower part of Figure 1. The result of the post processing is a set of filtered images and we denote the space of all filter images, generated by a given filter operator, by $\mathscr{F}$. As before the illumination change s induces a transformation s_f on the space $\mathscr{F}$.

The last component of our system is the characterization of images or filter images in terms of probability distributions or statistical descriptors (like means or moments) computed from these probability distributions. We denote the space of probability distributions (or the space of their descriptors) by $\mathscr{P}$ and $\mathscr{Q}$ for the images or the filtered images respectively. Here again the illumination operator s induces operators t_i and t_f on the spaces $\mathscr{P}$ and $\mathscr{Q}$.

Group Theoretical Structures

The general model presented in the last section describes the relation between illumination changes and induced changes in color images, filter images and spaces of descriptors is valid in general and does not take into account the fact that illumination changes are often described by curves in the space of illumination spectra. The main goal of this paper is the investigation of the question how the structure of the one-parameter curves in illumination space translates to the structure of the spaces of color images, filter images and probabilistic descriptor spaces. It is
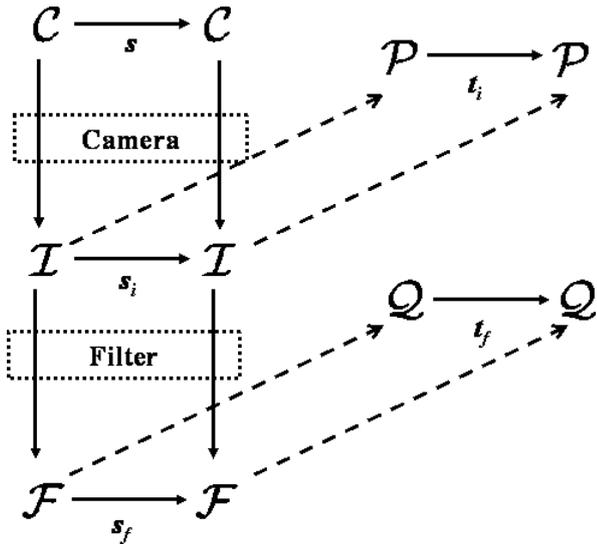
Figure 1. *Illumination changes and induced transforms of images, filtered images and their probabilistic descriptors*

(a) NCS colors   (b) Scene3   (c) Scene5

Figure 2. *Simulated RGB images for three multispectral images*

to describe properties of a collection of objects (like the pixels in an image) by their probability distribution. Probability distributions are, like spectral distributions, functions that can only assume non-negative values. From the general framework of function spaces of non-negative valued functions we know that the space of PCA coefficients of probability distributions also has a conical structure. After projecting sequences of probability distributions to a two-dimensional disk (corresponding to the chromaticity disk for spectral distributions) it is therefore possible to use the same SU(1,1) based methods to investigate the properties of these histogram-based sequences on the unit disk.

Experiments

In our experiments we use as illuminants sequences of black-body radiators in the mired-parametrization. Given the start temperature T_0, the end temperature T_N and the number $N+1$ of radiators in the sequence we denote the k-th element in the sequence by s^k as described in the previous section.

The behavior of the induced images and descriptors is highly dependent on the statistical properties of the sets of reflectance spectra of the object under consideration. In the following we will use three different objects to represent the different nature of important types of scenes. The first image is a simulated multispectral color checker. It consists of a collection of color patches defined by reflectance spectra from the NCS color atlas. The two other images are multispectral images measured by a multi-channel camera. The first image (named scene3) is an image of a natural outdoor scene while the second image (scene5) shows an indoor scene with man-made objects. The images are part of the collection described in [7]. As a camera model we use the estimated camera sensitivity functions of a consumer camera, a Canon EOS 10D. The methods used to derive these sensitivity functions are described in [8]. The simulated images of the three objects under neutral illumination (defined by a flat spectral distribution) are shown in Figure 2.

A typical distribution of the chromaticity coefficients for a sequence of black-body radiators and their group-theoretical approximations is shown in Figure 3. Here we used 30 black-body radiators from 3000K to 14000K in the mired sampling. This is the sequences of illuminants used in the following experiments.

In the first experiment we simulate a sequence of RGB images where the multispectral images describes the natural outdoor scene and the man-made indoor-scene, the camera used is the Canon EOS 10D and the illuminants are the 30 black-body radiators described above. This results in a sequence of 30 RGB images. All RGB vectors of an image under a given illumination are located in a cube. In the cube we introduce a new coordinate system with the diagonal as the first axis and the second and third axes perpendicular to the diagonal. This is achieved by applying the transformation:

$$(R, G, B) \mapsto \left(\frac{R+G+B}{\sqrt{3}}, \frac{R-G}{\sqrt{2}}, \frac{R+G-2B}{\sqrt{6}} \right)$$

very difficult to make some general observations since the effect of the illumination changes depends on the statistical characteristics of the collection of reflection spectra on which they operate. In the extreme case where the object points are all perfect black the illumination changes will have no effect. In the other extreme case where all reflectance spectra are perfect white reflectors we are back at the case of changing illumination spectra since the color signals are identical to the illumination spectra. Real scenes can therefore be expected to show a behavior somewhere between the extreme cases of no change at all and the one-parameter transformation rules observed previously.

In the following we will select sequences of black-body radiators as typical examples of changing illumination spectra. This choice was natural since black-body radiators are exactly defined by an equation that describes the spectral distribution as a function of the temperature. Earlier we have shown that such sequences can be described by one-parameter subgroups of the Lorentz-group SU(1,1) and that there is a close relation between the group parameter and the mired-parametrization of the black-body radiators. Also from a practical point of view black-body radiators are of interest since many color imaging software packages allow the user to manipulate color images with the help of a temperature parameter that links the current operation to black-body radiators of the given temperature.

With this selection we now have a sequence of illumination spectra $s(T)$ for a given sequence of temperatures $T_0, \ldots, T_N$. We always use the inverse temperature to define the increment between neighboring sources and we have thus: $1/T_{N-k} = 1/T_N + k\Delta$ where Δ is the fixed increment parameter. For given start- and end-temperatures T_0, T_N we write for the illumination spectra $s^k = s(T_k)$. For the other operators we choose a corresponding notation, i.e.: s_i^k for the image operators, s_f^k for the filter operators and t_i^k, t_f^k for the transformations in the probability-related spaces. We know from previous experiments that we can find Lorentz-transformations M_k such that $M_k \langle z_0 \rangle$ is a good descriptor of the chromaticity of the corresponding black-body radiator s^k. Since the M_k are a discrete sampling from a one parameter group we can find a matrix X such that $M_k = e^{kX}$.

Before we describe our experiments and the results in detail we have to mention another application of the Lorentz group SU(1,1) that will be used later. In many experiments we choose
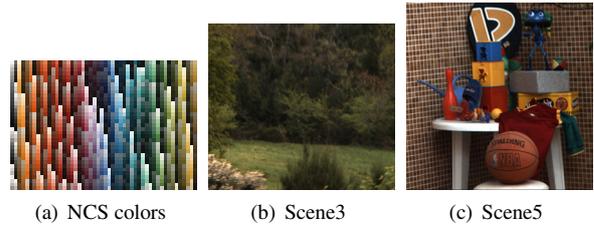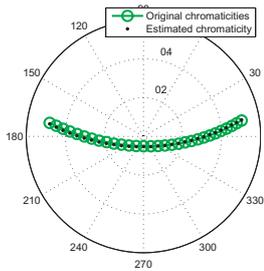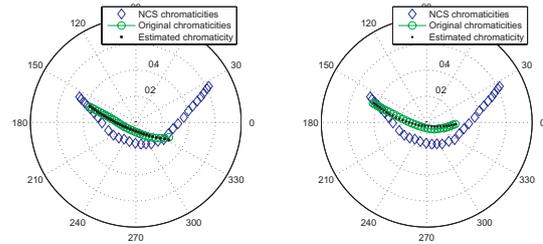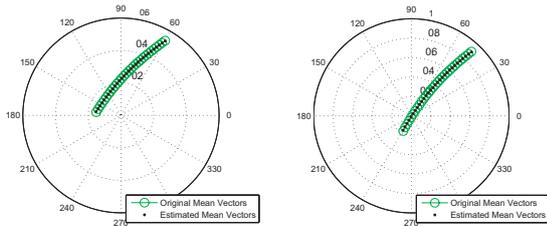
Figure 3. *Chromaticity coordinates: Planck spectra and approximations*

(a) Scene3   (b) Scene5

Figure 4. *Variation of mean vectors and approximations for scenes 3 and 5*

(a) Scene3   (b) Scene5

Figure 5. *Chromaticity coordinates from histograms and their approxima-tions for scene3 and scene5. Diamonds correspond to the position of the reference images calculated from the NCS atlas*

In this new coordinate system the cube becomes a double-pyramid with the black and the white point at the bottom and the top and we can view the points with coordinates $(\frac{R-G}{\sqrt{2}}, \frac{R+G-2B}{\sqrt{6}})$ as points of the unit disk. Describing the images with the mean values of the distribution of these vectors of an image we see that (the intensity-independent properties of) an image can be described by a point on the unit disk. In the framework shown in Figure 1 we have the following processing: A multichannel image is a point in the space $\mathscr{C}$, the image obtained by the camera is a point in the space $\mathscr{I}$ and the mean vector is an element of the space $\mathscr{P}$ which is the unit disk (or rather the interior of a regular six-sided polygon). The operator s is the pointwise multi-plication with the illumination spectrum, s_i describes the induced color change in the RGB image and t_i is a mapping of the unit disk by means of the mean vector of the $(\frac{R-G}{\sqrt{2}}, \frac{R+G-2B}{\sqrt{6}})$ points.

In Figure 4 the location of the mean vectors and the esti-mated SU(1,1) curve are shown for the two multichannel images. The locations of the points computed from the simulated images are shown by the green circles, the locations of the points ob-tained by the SU(1,1) approximation are the black points. We see that the mean vector curves generated by the illumination changes are very well approximated by the SU(1,1) approxima-tions. One interesting difference between the curves for the in-door and the outdoor scene is the radial scale in these two dia-grams. We see that the variation for the indoor scene is much larger than the variation for the outdoor scene. This is of course an effect of the larger variation of reflectance spectra in the in-door scene. It illustrates how scene properties influence the prop-erties of the mappings involved.

In the next experiment we characterize color images by their RGB-color histogram. The experiment consists of the following processing steps: we first compute the histograms for all (simu-lated) RGB images showing the NCS multispectral chart under the black-body illuminants mentioned above. Then we computed a PCA-basis in histogram space by computing the eigenvectors of this histogram set. This basis is then used in all further experi-ments (notice that coordinate vectors always depend on the basis selected to compute them). In the next step we then computed the RGB histograms for the simulated RGB images derived from the multispectral scenes (scene3 and scene5) under the same set of black-body illuminants. These histograms are described in the common coordinate system defined by the basis computed from the NCS chart. The camera model is always given by the esti-mated sensitivity functions of the Canon EOS 10D. Finally the PCA-coordinate vectors of the histograms are projected to the chromaticity disk in the same way as for the ordinary PCA co-ordinates of the spectra. As a result we get curves on the disc that we can analyze with the standard tools of group-theoretical regression. This is possible since probability distributions are functions with non-negative function values and we showed that such function spaces have a conical structure reflected in the con-ical distribution of the PCA expansion coefficient vectors.

Figure 5 shows the curves obtained for scene3 (the natural scene) and scene5 (the man-made scene). Again we use green circles for the points from the RGB histograms and black points are the group theoretical approximations of the green curve. As a reference curve (blue diamonds)we show the location of the points computed from the histograms of the NCS chart, defining the coordinate system used. We see that also in this experiment the group theoretically based regression gives a good approxima-tion of the original data.

The previous experiments show that the curve defined by an SU(1,1) one-parameter subgroup in the illumination space maps to related SU(1,1) curves in the spaces of the chromaticity part of the mean vector of the RGB images and the RGB histogram space. The form of the curves is given by the matrix X, the po-sition by the start point z_0 and the location on the curve by t (see Eqs. (5), (3) and (6)). From the definition $M_t = e^{tX}$ follows also that the pairs (t, X) and $(\gamma t, \frac{1}{\gamma}X)$ define the same matrix M_t for all non-zero constants γ. From this relation we obtain the following strategy for estimating the temperature of an illumi-nant in a sequence of black-body radiators: From the chromatic-ity descriptors (represented by the points on the unit disk) we compute the parameters of the matrix X and the parameter se-quence t_k. The distance between two illuminants is related to the difference between their t parameters and we can estimate the temperature based on these differences. These relations are illustrated in Figure 6. In these Figures select the point of the unit disk corresponding to the illuminant with the highest tem-perature. We compute then the distances of the other points on the unit disk as the accumulated sum of the t parameters along the corresponding SU(1,1) curve. For every description we ob-tain thus a mapping from the temperature of the illuminant to
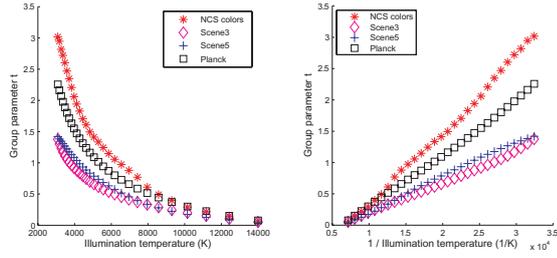
(a) Curve length as function of the color temperature of the illuminant

(b) Curve length as function of inverse color temperature of the illuminant

Figure 6. *Relation between curve length and the color temperature for the spectral description (Planck) and the RGB histogram descriptors computed from the NCS, scene3 and scene5 multi- spectral images*

a distance value. In Figure 6 we illustrate this mapping for the SU(1,1) description of the spectral distribution of the black body radiator (denoted by Planck) and the histogram descriptors computed from the RGB images of the NCS, scene3 and scene5 multispectral scenes measured by the Canon EOS 10D camera. In Figure 6(a) we use as x-axis the temperature scale whereas we use the inverse temperature as x-axis in Figure 6(b). From the figures we see that there is a linear relation between the color temperature in the mired parametrization and the curve length of the descriptors on the unit disk. For the PCA-based description of the spectral distribution this relation was observed before but this result shows that a corresponding linear relation also holds for the PCA-based description of RGB histograms of camera images. This simple relation between the group theoretical descriptions and the mired parametrization of color temperature is remarkable since perception-based color differences are also similar to the mired scale.

Next we include an linear filtering processing step and compute histograms of the resulting images. As an example we use the simplest version of a filter system based on the representation theory of finite groups (see [2, 1, 6]). These filters are based on the representations of the dihedral group D(4) as symmetry group of the grid and the representations of the permutation group S(3) as symmetry group of the color channels. In the simplest case (used here) the filter kernels have size 2x2 and a filter system consists of 12 filter functions. From the representation theory of the permutation group we find that the 2x2x3 (2x2 pixels with three RGB channels) RGB window is first recoded into the (R+G+B, R-B, G-B) combinations. The the following spatial filters are applied to each of these channels.

$$F_0 = \begin{pmatrix} 1 & 1 \\ 1 & 1 \end{pmatrix} \qquad F_1 = \begin{pmatrix} 1 & -1 \\ -1 & 1 \end{pmatrix}$$

$$F_2 = \begin{pmatrix} -1 & -1 \\ 1 & 1 \end{pmatrix} \qquad F_3 = \begin{pmatrix} -1 & 1 \\ -1 & 1 \end{pmatrix} \qquad (8)$$

We denote these filters by F_k^l where $k = 0, \ldots 3$ as above and $l = 0, 1, 2$ denote the $R + G + B, R - B, G - B$ combinations. It can be shown that they are the transforms of spatio-spectral images that correspond to the Fourier Transform for time signals. It is also known that the internal structure can be used to create fast implementations corresponding to the Fast Fourier Transform. Furthermore it can be seen from their definition that their computation requires only additions and subtractions. From the general theory follows also that the first two filters F_0, F_1 can be treated separately whereas the last two F_2, F_3, the horizontal and vertical edge filters should be treated as a pair. The filter results
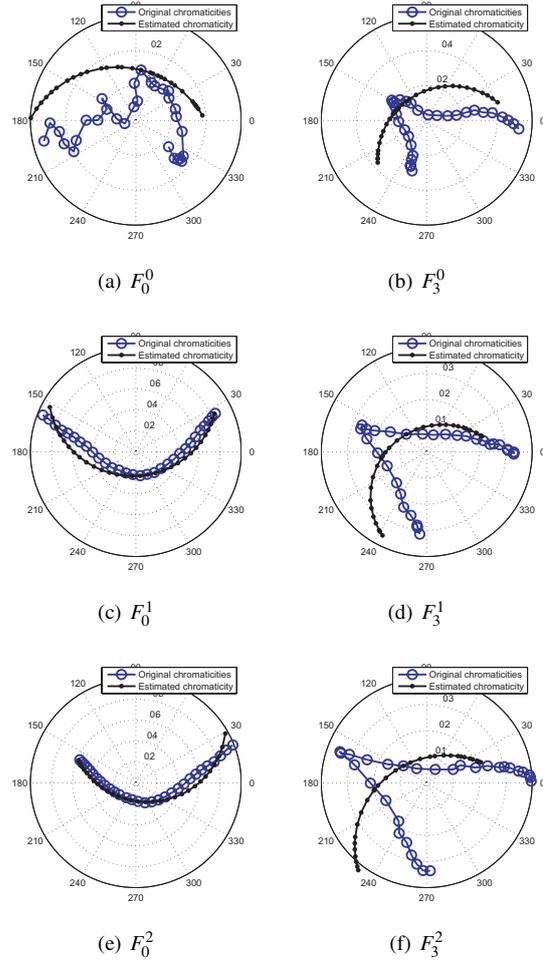
(a) F_0^0

(b) F_3^0

(c) F_0^1

(d) F_3^1

(e) F_0^2

(f) F_3^2

Figure 7. *Chromaticity coordinates for images filtered with (a) F_0^0, (b) F_3^0, (c) F_0^1, (d) F_3^1, (e) F_0^2 and (f) F_3^2*

obtained by applying these two filters should be re-coded and we will use the length and the angle between these pixel-wise, two-dimensional filter vectors. This is the well-known separation of edge-strength and orientation in low-level image processing.

Applying these filter systems to an RGB image results in 12 new images and together with the magnitude/angle recoding we obtain an 18-dimensional feature vector at each point in the image. We computed for each of these 18 images its histogram and generated thus for every RGB image series 18 new series of images together with their 18 histogram descriptions. For each of these histogram sequences we computed a PCA representation and described their contributions to the second and third eigenvector by points on the unit disk. Some plots of the sequences on these disks are provided in Figure 7. These plots were generated from the NCS color atlas. The sequences for six different filters are shown in Figure 7(a)-(f). The plots in the first column (a,c,e) are computed by a spatial smoothing of the intensity (R+G+B), the R-B and the G-B image. The second column (b,d,f) shows the result of the vertical gradient filter applied to the three images (R+G+B, R-B, G-B). For filters involving negative coefficients it can be seen that the filter response zero dominates the resulting histogram. We ignored the corresponding histogram bin in subsequent computations.

For the magnitude/angle results we took into account only pixels where the edge-strength was above a pre-defined threshold. For the remaining pixels in the image we computed the histograms and their representation in the PCA-coordinate system.
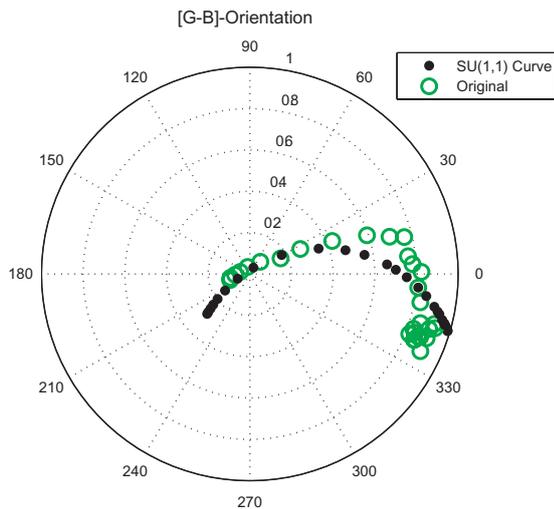
Figure 8. *(G-B) orientation locations and SU(1,1) curve approximation*
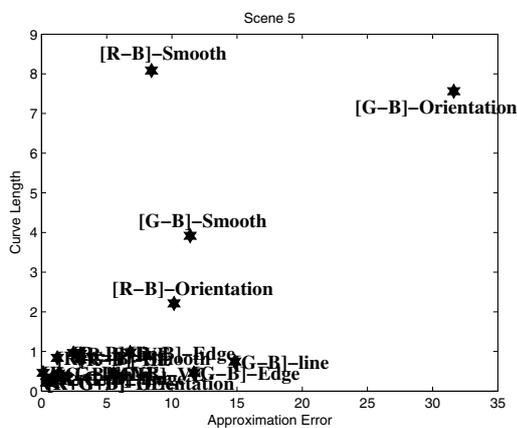

Figure 9. *Performance Evalutation for Scene 5*

The positions for the (G-B) orientations computed from Scene5 and the approximating SU(1,1) curve are shown in Figure 8. A visual inspection of the curves in Figures 7 and 8 has to take into account two factors: the length of the curves and the distance between the measured parameter points and the SU(1,1) curve. The variation for the spatial smoothing filters for the (R+G+B) image is relatively small (low values for the radius) while the variation for the corresponding filters for the (R-B) and (G-B) images is much larger. We therefore show in Figure 9 the curve lengths and the approximation errors (both computed based on the hyperbolic distance between points on the unit disk) of all the original filter results and the derived edge strength and edge orientations representations. We can see that the spatial smoothing of the (R-B) and (G-B) images and the orientation values computed from the (R-B) and (G-B) images are clearly superior to the other results since they produce curves on the unit disk that are significantly longer than the curves originating in the other filter results.

Conclusions

In this paper we showed that the SU(1,1) structure of the black body radiators in the space of illumination spectra maps to similar structures in certain spaces of statistical descriptors of RGB-images. We showed that this relation holds for the mean

of the RGB vectors and the PCA-coordinate vectors of RGB histograms. We also showed that PCA-coordinate descriptions of histograms of certain spatio-spectral filter result images follow the SU(1,1) curve structure to a large extent. Especially the filtered images computed from the (R-B) and (G-B) images show this relationship.

Acknowledgments

References

[1] R. Lenz. Investigation of receptive fields using representations of dihedral groups. *J. Vis. Comm. Im. Repr.*, 6(3):209–227, 1995.

[2] R.Lenz. Using representations of the dihedral groups in the design of early vision filters. In *ICASSP*, pages V165–V168. IEEE, 1993.

[3] R.Lenz. *Spectral Color Spaces: Their Structure and Transformations*, In *Adv. in Imaging and Electron Physics*, volume 138, pages 1–67. Elsevier, 2005.

[4] R.Lenz and T. H. Bui. Statistical properties of color signal spaces. *J. Opt. Soc. Am. A*, 22(5):820–827, 2005.

[5] R.Lenz, T. H. Bui, and J. Hernández-Andrés. Group theoretical structure of spectral spaces. *J. Math. Imaging and Vision*, 23:297–313, 2005.

[6] R.Lenz, T. H. Bui, and K. Takase. Fast low-level filter systems for multispectral color images. *Proc. AIC-05*, pages 535–538. Int. Color Ass., 2005.

[7] S.M.C. Nascimento, F.P. Ferreira, and D.H. Foster. Statistics of spatial cone-excitation ratios in natural scenes. *J.Opt. Soc. Am. A*, 19:1484–1490, 2002.

[8] M. Solli, M. Andersson, R.Lenz, and B. Kruse. Color measurements with a consumer digital camera using spectral estimation techniques. In *Proc. SCIA 2005*, *Springer LNCS 3540*, pages 105–114, 2005.

[9] S. Tominaga and B. A. Wandell. Natural scene-illuminant estimation using the sensor correlation. *Proc. IEEE*, 90(1):42–56, 2002.

[10] G. Wyszecki and W.S. Stiles. *Color Science*. Wiley & Sons, London, England, 1982.

Author Biography

Thanh Hai Bui *received the Ph.D. degree from the Department of Science and Technology, Linköping University, Sweden in 2005. He obtained his B.Sc. in Computer Science from Hanoi University of Technology in 1995, Post-graduate diploma in Manufacturing System Engineering from Asian Institute of Technology in 1999, Master of Applied Computer Science from Vrije Universiteit Brussel in 2000.*

Reiner Lenz *is associate professor at the Department of Science and Technology, Linköping University, Sweden. He received an diploma degree in mathematics from the Georg August Universität, Göttingen, Germany and a PhD degree in Electrical Engineering from Linköping University, Sweden. He received an honorable mention for the Pattern Recognition Society Award and is associated editor for Pattern Recognition and the IEEE-Transactions on Image Processing.*

Martin Solli *has a Master of Science in Media Technology and Engineering from Linköping University, Sweden, where he currently is working as a Ph.D. Student at the Department of Science and Technology. His research is focused on image databases and color signal processing.*